

DESIGN AND DEVELOPMENT OF A FLEXIBLE, CABLE-CONTROLLED AND HYPERREDUNDANT ROBOT WITH STRENGTH-ADJUSTABLE BALL JOINTS

Dominik Diek, Kemajl Stuja & Mohamed Aburaia



This Publication has to be referred as: Diek, D[ominik]; Stuja, K[emajl] & Aburaia, M[ohamed] (2022). Design and Development of a Flexible, Cable-Controlled and Hyper-redundant Robot with Strength-Adjustable Ball Joints, Proceedings of the 33rd DAAAM International Symposium, p. xxx-xxx, B. Katalinic (Ed.), Published by DAAAM International, ISBN 978-3-902734-xx-x, ISSN 1726-9679, Vienna, Austria
DOI: 10.2507/33rd.daaam.proceedings.xxx

Abstract

The universal industrial robot is the 6-axis articulated robot, which consists of six serially connected joints and has six degrees of freedom. Hyper-redundant robots have additional, redundant degrees of freedom thanks to additional serially connected link axes, resulting in increased flexibility that allows them to better manoeuvre curved paths. Hyper-redundant robots either feature precise control of each joint axis using only one actuator per joint or can be manipulated in at least two spatial directions in each joint axis. However, these single systems do not exhibit these two properties in combination. The goal of this work is to develop a concept in the form of a prototype that combines these features. By combining them, an optimization in terms of size and flexibility can be achieved. In this sense, a blocking (holding) system has been developed which is based on strength adjustable ball joints. The 3D-printed hyper-redundant robot is controlled by cables. To validate this system concept, after development of the kinematics and control of the robot, tests were carried out regarding the payload of a joint and the entire robot arm, with subsequent absolute accuracy testing of the robot arm. The results of this work in terms of the concept are presented in tabular form and discussed in detail. An outlook for future development is also given.

Keywords: hyper-redundant robot; strength adjustable ball joint; holding system; absolute accuracy; 3D printing.

1. Introduction

Industrial robots cannot be used for certain applications with special requirements. An example of this is inspections of rooms or rescue operations after a natural disaster (earthquake), when we are dealing with a destroyed, disorderly environment. Here the snake-like robots with several degrees of freedom (several axes) are used to move objects through the obstacles (curved paths). Against it, the industrial robot is the 6-axis articulated robot and consists of six serially connected link axes. Due to their arrangement, these six articulated axes allow the end effector a maximum degree of

freedom of six. Three degrees of freedom are required for obtaining the spatial position and three are required for orientation [1]. This means that the objects in the work area of the industrial robot can be manipulated in cartesian space.

On the other hand, the number of joint axes thus limits the maximum degree of freedom of the industrial robot. In contrast, hyperredundant robots have redundant degrees of freedom, resulting in an increase in flexibility that gives them the ability to manoeuvre curved paths. The resulting kinematic redundancy enables robots of this type to achieve a pose in multiple robot configurations [2]. Applications for robots of this class can be found, for example, in surgery, cleaning and inspection operations, and as manipulators during rescue operations [3].

To expand these application areas, an optimization regarding size and flexibility is to be carried out in the course of this work. The joint axes of the hyperredundant robot should be individually controllable in two degrees of freedom, using only one actuator per joint. The design process is based on the V-model according to VDI 2206 [4] and methodical approach is related to works [5] and [6]. After the conceptual design of a holding system that meets the requirements of the mechatronic system, a 3D-printed prototype of the robot is created based on this, so that the elaborated concept, which enables the individual control of joint axes, can be tested, and validated too.

2. Problem Statement – Materials and Methods

Hyperredundant robot systems either have precise control of each joint axis or can be manipulated in at least two spatial directions in each joint axis. However, these individual systems do not exhibit these two characteristics when only one actuator per joint axis is used. The aim is to investigate how these features can be combined so that flexible control of the kinematic structure can be realized with maximum reduction of active components or actuators, both in the robot base and directly on the manipulator. The reduction of installed actuators should extend the range of application, entail financial savings, and positively influence flexibility and size.

2.2. Design of the holding system and the hyperredundant robot

The designed hyperredundant robot (see Figure 1 left) is cable-controlled and consists of a kinematic chain of four strength-adjustable ball joints connected in series (see Figure 1 right). The robot base is the static part of the system that houses the electronics, pneumatics, and motors. There are three motors whose flanges are wrapped cables that run through holes in all joints of the robot (see the figure 3 für better understanding). The 3 holes on joints are designed symmetrically at 120 degrees. The dynamic part of the system is the manipulator. The working area of the robot is the area outlined with blue colour. At the end of the kinematic chain is tool centre point (TCP). Sectional view of the joint is shown at the right side. When pressure is applied, a pneumatic short-stroke cylinder presses a stop buffer made of elastomer against the joint head. The resulting friction causes the joint to lock. By blocking all joints except the one to be manipulated, an individual control of a joint can be achieved by the hyperredundant robot. When tightening or loosening the ropes attached to the TCP, only the deblocked joint is manipulated due to the freedom of movement.

2.2 Design of the hyperredundant robot

The cables or steel ropes are wound or unwound in the base of the robot by three stepper motors. Figure 2 shows the chain of relationships for determining the forward kinematics. The motor steps change the cable lengths. This change influences the respective change of the joint angles of the joint to be controlled, which determines the pose of the end effector.

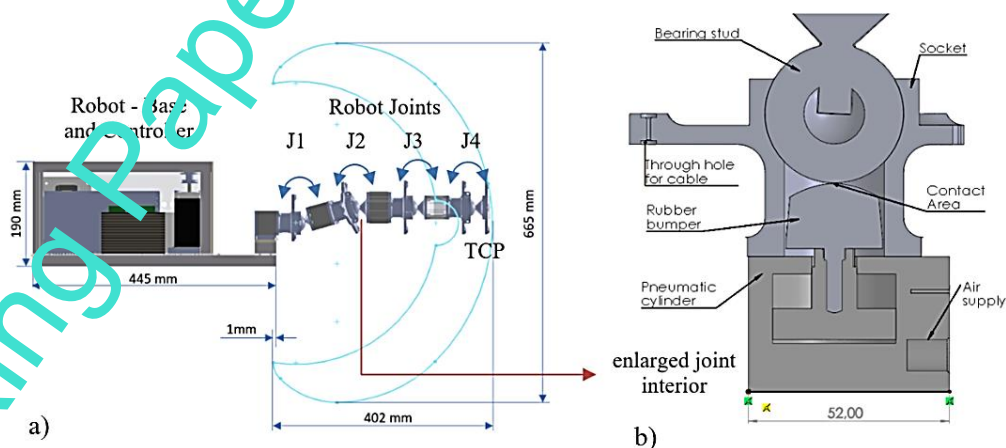


Fig 1. Hyperredundant robot work area (a) and sectional view of the joint with pneumatic cylinder (b) to illustrate the principle of holding

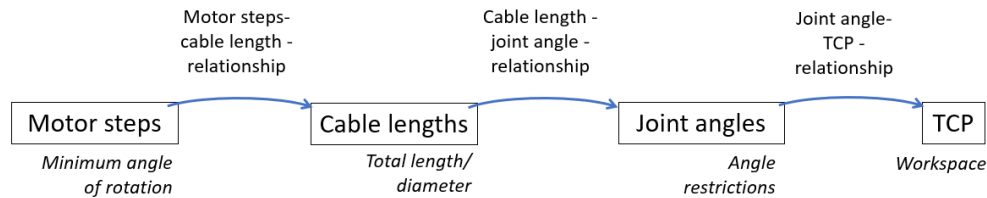


Fig. 2. Relations and limitations for the realization of forward kinematics

The prototype will be subjected to tests on load-bearing capacity and absolute accuracy. For its execution, the control is implemented based on the models of the calculations from the forward kinematics using DH table [7]. These joint angles are calculated similarly to the concept of Xu [8] based on the rope lengths between the joints and then transferred to the corresponding number of motor steps. By constructing the through hole for the cable at the height of the rotary axis of the bearing stud the construction space could get minimized.

3. Design of experiments, results and discussion

To perform the tests, the prototype (cf. Fig. 3) of the robot is needed, as well as a digital and a more sensitive analog force gauge. In addition, length measuring instruments (here: rulers) are required for measuring the TCPs of different configurations. The payload of the robot depends on the applied air pressure and is 1.5 kg at 10 bar. With a dead weight of the robot arm of 1.3 kg, a high power-to-weight ratio can thus be defined.

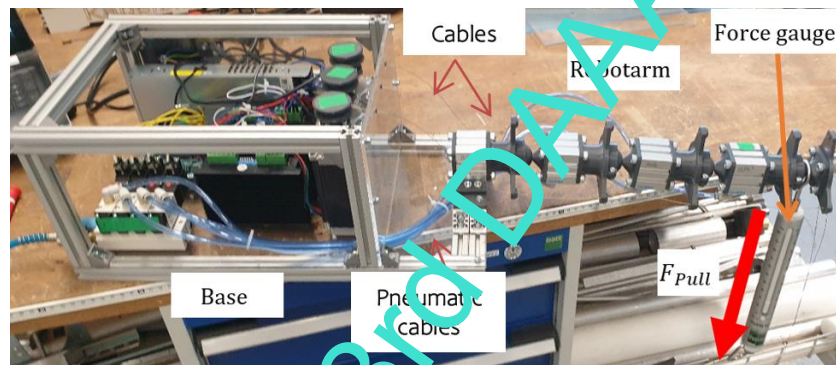


Fig. 3. Prototype and test setup for the investigation of the maximum payload in the stretching position

For the validation of the developed strength-adjustable ball joint, Figure 4 shows the experimental setup to determine the maximum load on it and Table 1 shows the values of the resulting friction coefficients.

As a result of the tests, the mean values of the ratios (coefficient of static friction) of applied force (measured tensile force) to piston force are relatively constant at 0.54 (softer elastomer: 45 Shore A) and 0.47 (harder elastomer: 60 Shore A). For rotations about the longitudinal axis of the socket, these ratios decrease by 0.21 and 0.34, respectively, due to distortions in the material under load. Accordingly, the softer elastomer achieved higher coefficients of friction in the series of measurements and is therefore more suitable for this robot application. During the tensile test at 8.0 bar and the stop buffer of the 45 Shore A material, the material failed at the 9.2 mm thick taper, resulting in separation of the ball. Thus, 339.2 N can be considered as the maximum load (without torsion) of the ball joint.

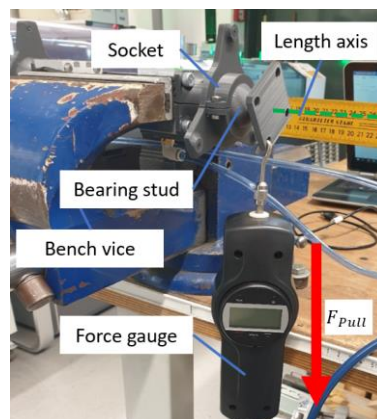


Fig. 4. Test setup for the investigation of the maximum payload of the ball joint

Air pressure [bar]	Piston force [N]	Applied force [N]		Torque [Nm]		Coefficient of static friction	
		45 Shore A	60 Shore A	45 Shore A	60 Shore A	45 Shore A	60 Shore A
0.0	0,0	0,0	0,0	0,00	0,00	0,00	0,00
0.5	40,2	2,0	0,0	0,07	0,00	0,05	0,00
1.0	80,4	30,7	27,6	1,01	0,91	0,38	0,34
1.5	120,6	77,7	74,1	2,56	2,45	0,64	0,61
2.0	160,8	96,7	90,0	3,19	2,97	0,60	0,55
2.5	201,1	112,5	106,3	3,71	3,51	0,56	0,53
3.0	241,3	137,6	126,4	4,54	4,17	0,57	0,52
3.5	281,5	148,6	142,4	4,90	4,70	0,53	0,51
4.0	321,7	164,7	155,2	5,44	5,12	0,51	0,48
4.5	361,9	191,7	172,4	6,33	5,69	0,53	0,48
5.0	402,1	230,6	190,0	7,61	6,27	0,57	0,47
5.5	442,3	240,5	201,7	7,94	6,66	0,54	0,46
6.0	482,5	248,7	229,8	8,21	7,58	0,52	0,48
6.5	522,8	293,3	247,4	9,68	8,16	0,56	0,47
7.0	563,0	295,4	237,1	9,75	7,32	0,52	0,42
7.5	603,2	329,6	240,7	10,88	7,94	0,55	0,40
8.0	643,4	339,2	241,6	11,19	7,97	0,53	0,38

Table 1. Maximum load for a strength-adjustable ball joint for rotations orthogonal to the longitudinal axis

To understand the kinematics and motion of the hyperredundant robot, the manipulator was placed in different configurations. Figure 5 shows 10 different configurations of the robot. Depending on how the 3 motors move (which of 3 cables is pulled or released) and by selectively blocking axes, different configurations can be approached. For example, Figures 1 and 4 show the movement of the first axis. Figures 2, 3 and 5 show the movement of the second axis. Figures 8 and 9 show the movement of all axes.

To control the movement of robot is necessary to synchronize the movement of motors and with switching on/off the pneumatic. The inverse kinematics was not done in this work; therefore, no statement can be made here about the positioning accuracy, trajectory accuracy and other important characteristics for the qualification of robots. This task then remains to be done for the future.

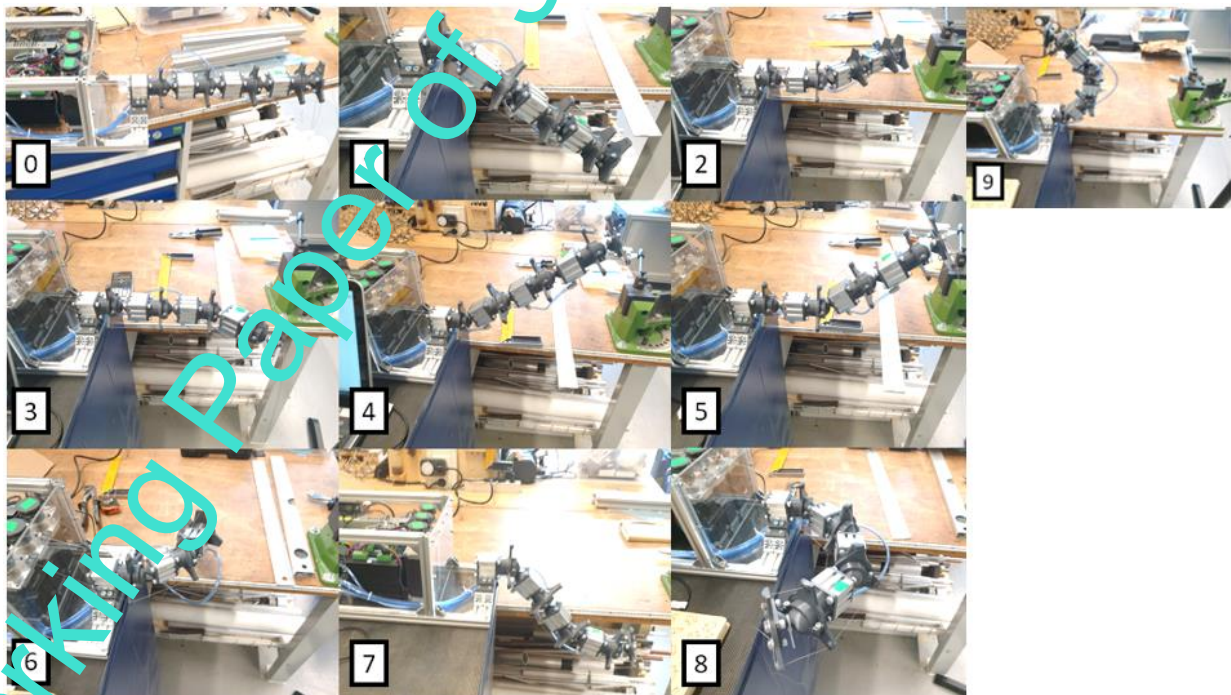


Fig. 5. Moving robot to different configurations.

4. Summary, conclusion and outlook

The design of a hyperredundant robot is a very extensive engineering task. To find an optimal design and a creative solution for this kind of robot kinematics, both a methodical approach and different software tools are required. In this work, a well-known methodological approach of VDI-2206 for the design of mechatronic systems was used. This methodological approach allows to use the creativity of the user to find different solutions for subsystems of the robot. From the different partial solutions, the best solution was selected for the design of the robot links/joints according to the requirements.

The main part of hyperredundant robot is the “holding system”, which enables robot to remain in the achieved position- axes configuration. The holding system accurately provides the blocking of all joints except the one to be actuated, was solved with the aid of strength-adjustable ball joints. A link consists of a pneumatic cylinder, a stop buffer, the 3D-printed joint socket and bearing stud. The base of the joint socket is a hollow cylinder, which allows the stop buffer bolted to the pneumatic cylinder to press against the joint head via this cavity. Based on this, a prototype was built to allow validations to be completed. The kinematic model was created, and the calculations based on it for the forward kinematics and the determination of the rope length as well as the corresponding motor steps were implemented for the control system.

To improve the design and functionality of strength-adjustable ball joints a real test stand stations were built. On test stand robots were driven with different movement parameters to validate the presumptions of friction model. These parameters and results are presented tabular in this work. This experiment has shown that the robot can lift its own weight and act flexibly with the aid of one built-in actuator per joint. The fully functional, flexible, cable-controlled and hyperredundant robot with strength-adjustable ball joints confirms the theoretical concept and fulfils the requirements that were defined based on the objective.

However, during experiments with real robots, it was found that specific components have potential for further optimization. Optimization approaches exist in the surface processing of the 3D-printed parts. The principal solution is based on the friction of components; therefore, the surface condition of contacted surfaces is very important. Clean Surface reduces the pressure needed to block (hold) the robot joints, prolong the life of components and are more energy efficient.

Further research should focus on realistic use cases with mounted grippers or cameras on the end effector. Further, the robot should be tested outdoors to see if the robot structure is negatively affected by environmental parameters such as temperature, humidity, etc. The inverse kinematics and the dynamics of flexible robot axes will be worked out to qualify the robot for different applications.

5. Acknowledgments

Our special thanks go to the University of Applied Sciences Vienna -FH Technikum Wien- for providing the equipment and the laboratory as well as for sponsoring this work. Furthermore, we would like to thank the colleagues of the engineering departments for their support.

6. References

- [1] Bender, D. G. B. (2020). *Dubbel Taschenrechner für den Maschinenbau 2: Anwendungen*, Springer Berlin Heidelberg, 978-3-662-59712-5, Berlin.
- [2] Rost, S. (2016). *Entwurf, Analyse und Regelung einer kinematisch redundanten Roboterstruktur mit hydraulischen Antrieben variabler Nachgiebigkeit*, Ph.D. Dissertation, Department of Electrical Engineering, Information Technology, Physics, Technische Universität Carolo-Wilhelmina zu Braunschweig, Braunschweig, Germany.
- [3] Tang, L.; Wang, J.; Zheng, Y.; Gu, G.; Zhu, L. & Zhu, X. (2017). Design of a cable-driven hyper-redundant robot with experimental validation, *International Journal of Advanced Robotic Systems*, Vol. 14, No. 5, pp. 1-12, DOI: 10.1177/1729881417734458.
- [4] Ponn, J & Lindenmann, U. (2011). *Konzeptentwicklung und Gestaltung technischer Produkte*, Springer Berlin Heidelberg, 978-3-642-20579-8, Berlin.
- [5] Stuja, K.; Katalinic, B.; Aburaia, M. & Pajaziti, A. (2021). Design of a Robot Application with Regard to Energy Efficiency, *Proceedings of the 32nd DAAAM International Symposium*, pp.0033-0039, B. Katalinic (Ed.), Published by DAAAM International, ISBN 978-3-902734-33-4, ISSN 1726-9679, Vienna, Austria.
- [6] Stuja, K.; Pajaziti, M., Markl E. & Aburaia, M. (2016). Lightweight 4 -Axis Scara Robot for Education and Research, *Proceedings of the 27th DAAAM International Symposium*, pp. 0102-0108, B. Katalinic (Ed.), Published by DAAAM International, ISBN 978-3-902734-08-2, ISSN 1726-9679, Vienna, Austria.
- [7] Denavit, J. & Hartenberg, R. S. (1955). A Kinematic Notation for Lower-Pair Mechanisms Based on Matrices, *Journal of Applied Mechanics*, Vol. 22, No. 2, pp. 215–221, DOI: 10.1115/1.4011045.
- [8] Xu, W.; Liu, T. & Li, Y. (2018). Kinematics, Dynamics, and Control of a Cable-Driven Hyper-Redundant Manipulator, *IEEE/ASME Trans. Mechatron.*, Vol. 23, No. 4, pp. 1693–1704, DOI: 10.1109/TMECH.2018.2842141.